



## The Influence of Weak Ionic Interactions on Electrode Reactions during Electrodeposition of Re-Ni Alloys

O. Berkh,<sup>a</sup> A. Khatchatourians,<sup>b</sup> N. Eliaz,<sup>c,\*</sup> and E. Giladi<sup>d,\*\*</sup>

<sup>a</sup>Department of Physical Electronics, Faculty of Engineering, Tel Aviv University, Ramat Aviv 6997801, Israel

<sup>b</sup>The Center for Nanoscience and Nanotechnology, Tel Aviv University, Ramat Aviv 6997801, Israel

<sup>c</sup>Department of Materials Science and Engineering, Faculty of Engineering, Tel Aviv University, Ramat Aviv 6997801, Israel

<sup>d</sup>School of Chemistry, Faculty of Exact Sciences, Tel Aviv University, Ramat Aviv 6997801, Israel

The electroplating of Re-Ni alloys in citrate electrolytes of different compositions was studied by cyclic voltammetry and by anodic stripping voltammetry, following galvanostatic deposition. The faradaic efficiency of the deposition process and the composition of the deposits were determined. Increasing the concentrations of either the nickel or the perrhenate ion in the electrolytes was shown to enhance the rate of deposition of the Re-Ni alloy. The process is influenced by mass transport and by concentration of citric acid in the electrolytes. Conductometry, UV-Vis and Raman spectroscopy were used for studying the ionic interactions in electrolytes. No evidence of the existence of perrhenate complexes with other components of the electrolyte was found. However, an increased deformation of the perrhenate ions with increasing molar ratio of  $[\text{NiCit}]^-/\text{ReO}_4^-$  was clearly shown by Raman spectroscopy. Hence, a weak interaction is definitely observed, which is enough to distort the shapes of the  $\text{ReO}_4^-$  and  $[\text{NiCit}]^-$  or  $[\text{NiHCit}]$  species, thus enhancing the deposition rate of the Re-Ni alloy. The induced co-deposition is believed to be a catalytic process, including the stage of simultaneous reduction of  $\text{ReO}_4^-$  and  $[\text{NiCit}]^-$  or  $[\text{NiHCit}]$  species, which influences each other by weak interaction.  
© 2014 The Electrochemical Society. [DOI: 10.1149/2.0071412jes] All rights reserved.

Manuscript submitted May 5, 2014; revised manuscript received July 11, 2014. Published August 12, 2014.

Rhenium and its alloys are used for different purposes where stability at high temperatures is important, such as aerospace and nuclear industries, as well as in catalysis, mainly for the petroleum industry. It also has applications as coatings. We have published a detailed listing of its unique properties and applications.<sup>1</sup> Electrodeposition of Re itself is very difficult, and the resulting deposits are usually non-uniform and tend to peel off readily. However, addition of the salts of Ni, Co or Fe catalyzes the deposition of the respective alloys. A typical plating bath consists of  $\text{ReO}_4^-$ ,  $\text{Ni}(\text{SO}_3\text{NH}_2)_2$  and citrate.<sup>2-10</sup> The mechanism of induced co-deposition of Re with one of the above iron-group metals has been studied recently in our research group,<sup>5-8</sup> with emphasis on the role of Me (Me = Ni, Co, or Fe). The composition of the alloy deposited could be controlled by the relative concentration of the three components of the bath, the pH of the solution, the temperature and the current density applied. The highest Re-content achieved was 93 at.% and the highest faradaic efficiency (FE) was 96% in different compositions of the baths in the above publications. A leading role of freshly deposited Ni in catalytic deposition of Re was observed.<sup>5-8,11</sup> On the other hand, a simultaneous discharge of Ni and perrhenate ions was shown to be responsible for the increase in the partial current density of the Re deposition.<sup>4</sup> The concept of simultaneous discharge is supported by the active role of perrhenate in nickel co-deposition. In fact, no Ni is deposited from the Ni electrolytes with high citrate to  $\text{Ni}^{2+}$  molar ratio (of about 4.2),<sup>12</sup> while about 20 at.% Ni is found in the deposits produced in electrolytes with the same citrate to  $\text{Ni}^{2+}$  molar ratio in the presence of 34 mM perrhenate.<sup>5</sup> According to our results, the FE of deposition in an electrolyte containing 100 mM citric acid and 94 mM Ni sulfamate did not exceed 26%, while in the presence of 34 mM  $\text{NH}_4\text{ReO}_4$  the partial FE of Ni deposition was near 60%.<sup>13</sup> In a recent work,<sup>14</sup> it was shown that the FE of the deposition process in an electrolyte containing 34 mM citric acid and 94 mM Ni sulfamate increased from 10% to 57% with increasing  $\text{NH}_4\text{ReO}_4$  concentration in the range of 1–100 mM.

In a recent publication,<sup>13</sup> we studied the initial stages of deposition of Re-Ni alloys. Following galvanostatic electrodeposition, an anodic linear sweep was applied, and the charge consumed in stripping was calculated. The FE was obtained as the ratio of the anodic to cathodic charges measured. Experiments conducted in this manner at a deposition time of 2 s yielded a surprising FE = 220%, and at even shorter deposition times much higher values of the FE were observed. This

behavior was discussed in details in our recent publication.<sup>13</sup> The anomalously high values of the FE can be explained by assuming that reduction of the two metals forming the alloy may occur along two parallel paths: electrodeposition and chemical reduction. Although this is not common, it had been reported in the literature.<sup>15-18</sup> Both the FE and the Re content in the alloy declined with increasing deposition time. It should be emphasized that the combination of all three components in the electrolytes are required in order to observe the above phenomena.<sup>13</sup>

Based on the cited results,<sup>4,5,12-14</sup> one could suggest simultaneous electrodeposition of Re and Ni facilitated by interaction of perrhenate, nickel and citrate species in electrolyte. The concept of perrhenate and citrate interaction with formation of a reversible electroactive perrhenate/citrate complex ( $\text{H}_2\text{CitReO}_4$ )<sup>2-</sup> was utilized in the explanation of the catalytic influence of citrate on the reduction of  $\text{ReO}_4^-$  in mildly acid electrolytes which was shown by polarographic studies. On the other hand, UV-Vis spectroscopy did not confirm the formation of the complex, probably because of its low stability.<sup>19</sup> The cyclic voltammetry tests on copper electrodes indicated that citric acid does not catalyze the reduction of perrhenate ions.<sup>11</sup> This apparent inconsistency can be attributed to the stronger interaction of carboxylic groups with copper than with  $\text{ReO}_4^-$ . As a consequence, the solid copper surface can be blocked by citrate. In contrast, the mercury electrode surface in polarography is periodically renewed, preventing blocking of the surface.

Ionic interaction in the electrolytes for deposition of Re-Ni alloys has not been studied so far, with the exception of reference 11, in which the formation of citrate-perrhenate complex was discarded based on the data of UV-Vis spectroscopy while formation of nickel-citrate complexes was confirmed.

The aim of the present work is to shed further light on the problem of the mechanism of induced co-deposition of Re-Ni alloys from electrolytes containing citrate. We studied the deposition of Re-Ni in stagnant and stirred electrolytes of different compositions at different deposition times and pH. The observed features of the process were considered in terms of simultaneous rhenium and nickel deposition as a result of weak ionic interaction in electrolytes. The interaction of  $\text{ReO}_4^-$  and  $\text{Ni}^{2+}$ -citrate in the electrolytes used for deposition of Re-Ni alloys was studied using Conductometry, UV-Vis and Raman spectroscopy.

### Experimental

Electrodeposition was carried out from electrolytes containing 34–130 mM nickel sulfamate and 10–50 mM ammonium perrhenate. Two

\*Electrochemical Society Active Member.

\*\*Electrochemical Society Fellow.

†E-mail: neliaz@eng.tau.ac.il

concentrations of citric acid, 340 mM and 100 mM, were studied. The pH of the electrolytes was adjusted to a value of  $5 \pm 0.1$  (unless otherwise indicated) with 5 M NaOH solution. A few experiments were conducted at  $\text{pH } 3 \pm 0.1$ , for comparison.

Cyclic voltammetry, galvanostatic deposition and linear sweep anodic stripping experiments were conducted at  $70 \pm 1^\circ\text{C}$  in standard three-electrode cells (Metrohm) with Pt-foil counter electrodes and saturated calomel reference electrode (SCE). A potentiostat/galvanostat (model 273, Applied Research) was used. All potentials were measured and reported relative to SCE. The potential scan rate in all potentiodynamic experiments was  $50 \text{ mV s}^{-1}$ . For studying the effect of mass transport on the deposition process, galvanostatic experiments were conducted in both stagnant and stirred electrolytes. A magnetic stirrer was used for stirring.

For cyclic voltammetry experiments, gold disk working electrodes (area  $0.1 \text{ cm}^2$ ) were used. They were polished before each scan with Buehler polishing cloth and a suspension of alumina powders with particle size of  $0.3 \mu\text{m}$ , rinsed with deionized water and cycled in  $0.5 \text{ M H}_2\text{SO}_4$  in the range of  $0-1.6 \text{ V}$  in order to obtain reproducible voltammogram. The Au electrode was faced toward the bottom of electrochemical cell (as in a Rotating Disk Electrode) during cyclic voltammetry. The initial, reverse and final potentials were open circuit,  $-1.0 \text{ V}$  and  $+0.5 \text{ V}$ , respectively.

The deposition and anodic stripping of Re-Ni deposits were done on vertically arranged Pt electrodes with an area of  $0.12 \text{ cm}^2$ . Preparation of the Pt electrodes for deposition was carried out in  $0.5 \text{ M H}_2\text{SO}_4$ , cycling the potential from  $-0.2 \text{ V}$  to  $+1.6 \text{ V}$ , until a reproducible pattern was obtained.

The FE of the deposition process was calculated as the ratio of charge measured in linear anodic stripping of the deposit and the charge consumed during deposition. Deposition was conducted at  $50 \text{ mA cm}^{-2}$  for 2–300 s. Stripping was conducted by linear sweep of potential from open-circuit potential to  $+1.1 \text{ V}$ , in the same electrolyte where deposition was conducted.

For comparison of the initial and following stages of deposition, the deposition was carried out for times as high as 900 s on Cu foil cathodes. In these experiments, the FE was determined by weight gain following deposition, taking into account the electrochemical equivalent, calculated on the basis of the composition of the deposit. The composition of the deposits was determined by energy dispersive X-ray spectroscopy (EDS) analysis using a JSM-6300 scanning electron microscope (SEM) equipped with an Oxford EDS detector.

The UV-Vis spectra were recorded at room temperature using a Cary 100 Varian Spectrophotometer. Spectra were recorded in the range of 200–850 nm. The conductivity of the electrolyte was measured using a laboratory bench-top pH/mV/Cond./TDS/Temp meter 86505 (AZ Instrument Corporation, Taiwan). The accuracy and resolution of the measurement were  $\pm 1\%$  and  $0.05\%$  (of full scale,  $0-200 \text{ mS cm}^{-1}$ ), respectively. The pH was measured using pH/mV/Temp Meter PL-600 with accuracy of  $\pm 0.01$  and resolution of  $0.01 \text{ pH}$ .

Raman spectroscopy measurements were performed with Horiba Jobin Yvon Raman spectrometer, model LabRam HR VIS-NIR. The laser line used was  $532 \text{ nm}$ . The laser illumination was focused into a Petri dish with the investigated solution using a long ( $14 \text{ mm}$ ) working distance Nikon LMPlan FL N objective,  $\times 50$ , N.A.  $0.5$ . The laser power of the objective was  $8 \text{ mW}$ . The grating used was  $600 \text{ lines/mm}$ . The acquisition time was a function of the signal strength obtained.

## Results and Discussion

**Cyclic voltammetry.**—Cyclic voltammetry measurements were conducted in electrolytes containing  $340 \text{ mM}$  citric acid. The concentrations of  $\text{ReO}_4^-$  and  $\text{Ni}^{2+}$  varied in the ranges of  $10-50 \text{ mM}$  and  $34-130 \text{ mM}$ , respectively. The voltammograms in the cathodic branches had poor reproducibility, probably because of intensive hydrogen evolution and bubble formation under a vertical electrode. The typical anodic branches of voltammograms are shown in Fig. 1a. The charge consumed in anodic stripping represents the amount of the

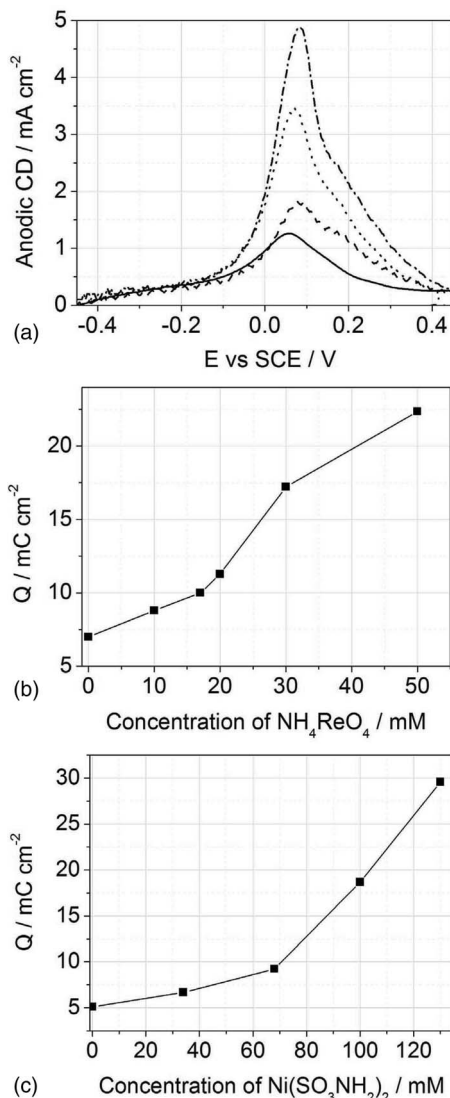


**Figure 1.** The effect of  $\text{NH}_4\text{ReO}_4$  and  $\text{Ni}(\text{SO}_3\text{NH}_2)_2$  concentrations on deposition of Re-Ni alloys. (a) Cyclic voltammograms (anodic branches); electrolytes contain  $340 \text{ mM}$  citric acid,  $94 \text{ mM}$   $\text{Ni}(\text{SO}_3\text{NH}_2)_2$  and different concentrations of  $\text{NH}_4\text{ReO}_4$ , —  $10 \text{ mM}$ ; ---  $20 \text{ mM}$ ; .....  $30 \text{ mM}$ ; - . - .  $50 \text{ mM}$ . (b) Charge calculated from anodic branches of the voltammograms vs. the concentration of  $\text{NH}_4\text{ReO}_4$ . Electrolytes as in 1a. (c) Charge extracted from anodic branches of the voltammograms vs. the concentration of  $\text{Ni}(\text{SO}_3\text{NH}_2)_2$ . Electrolytes contain  $340 \text{ mM}$  citric acid and  $34 \text{ mM}$   $\text{NH}_4\text{ReO}_4$ , and different concentrations of  $\text{Ni}(\text{SO}_3\text{NH}_2)_2$ .

deposited material. Figures 1b and 1c show the values of the charge calculated from the anodic branches of the voltammograms as a function of  $\text{ReO}_4^-$  and  $\text{Ni}^{2+}$  concentrations, respectively. The deposition of alloys was intensified both with increase the concentration of  $\text{ReO}_4^-$  (Figs. 1a and 1b) and  $\text{Ni}^{2+}$  (Fig. 1c) ions. It should be emphasized that a barely noticeable deposition was observed from electrolytes containing  $340 \text{ mM}$  citric acid and only perrhenate or only nickel salt. The results presented in Fig. 1 show a strong catalytic effect of both  $\text{ReO}_4^-$  and  $\text{Ni}^{2+}$  on the alloy deposition in citrate electrolytes.

The Re-content can reach more than  $90 \text{ at.}\%$ , while no complex with  $\text{ReO}_4^-/\text{Ni}^{2+} \geq 9$  can be considered.<sup>5</sup> Therefore, it is impossible to explain the deposition of Re-Ni alloys only by formation of a complex including citrate,  $\text{ReO}_4^-$  and  $\text{Ni}^{2+}$ . On the other hand, a complex with a  $\text{ReO}_4^-$  to  $\text{Ni}^{2+}$  ratio of 1 or 2 can be considered as a precursor for the partial deposition, from which a catalyst forms in the cathodic process. Additionally, rhenium and nickel can be deposited

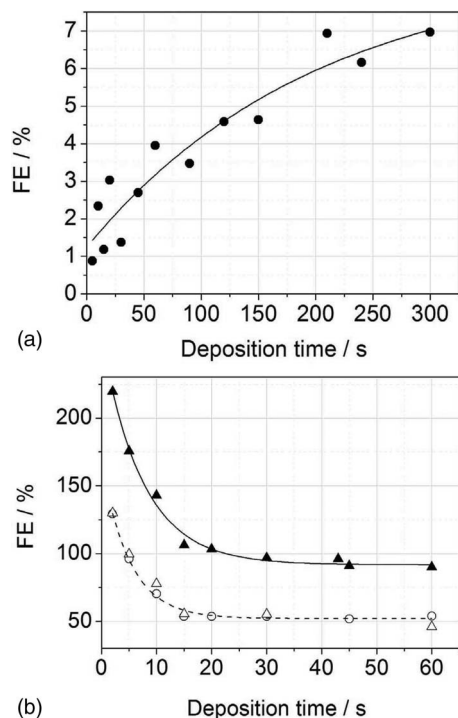


**Figure 2.** Anomalous faradaic efficiency (AFE) vs. deposition time for stirred and stagnant electrolytes, containing 94 mM  $\text{Ni}(\text{SO}_3\text{NH}_2)_2$ , 34 mM  $\text{NH}_4\text{ReO}_4$ , and different concentrations of citric acid. (a) Stirred electrolyte, 340 mM citric acid. (b) Stagnant electrolyte containing 340 mM citric acid ( $\circ$ ). Electrolytes containing 100 mM citric acid: stirred ( $\blacktriangle$ ) and stagnant ( $\triangle$ ).

in parallel to the deposition of a Ni-Re alloy. The prevailing process is determined mostly by the conditions of deposition. This concept seems to be suitable for the explanation of the effect of mass transport on the anomalous faradaic efficiency (AFE) and its dependency on the deposition time.

*The effect of mass transport on the deposition process at its initial stages.*— The effect of mass transport was determined by comparing results obtained in stagnant and stirred electrolytes of identical compositions. The effect of stirring on the time dependency of AFE for the Re-Ni deposition in two electrolytes with different concentrations of citric acid is shown in Fig. 2. The very low FE (of a few percents), which increases with deposition time, was observed for a stirred electrolyte containing 340 mM citric acid, 94 mM  $\text{Ni}(\text{SO}_3\text{NH}_2)_2$ , and 34 mM  $\text{NH}_4\text{ReO}_4$  (Fig. 2a). The AFE decreased from about 125% to 55% when the deposition time increased from 2 s to 30–60 s for a stagnant electrolyte of the same composition (Fig. 2b).

The effect of mass transport on the AFE for deposition in an electrolyte containing 100 mM citric acid, 94 mM  $\text{Ni}(\text{SO}_3\text{NH}_2)_2$  and 34 mM  $\text{NH}_4\text{ReO}_4$  is also presented in Fig. 2b. The results obtained in the stagnant electrolytes are almost the same as in the stagnant electrolytes with 340 mM citric acid, while the AFE decreased from about 220% to 95% when the deposition time was increased from 2 s to 60 s for stirred electrolytes.

As it was shown in our recent work,<sup>13</sup> the FE exceeds 100% in different electrolytes and under different experimental conditions at short deposition times and declines with deposition time. This behavior is characteristic of Re-Ni alloy deposition, and was not observed in deposition of Ni or Re separately. The FE exceeding 100% shows that a chemical reaction is taking place, in parallel with the electrochemical deposition of the Re-Ni alloy. However, no reaction was taking place until the deposition current was turned on. We believe that the shift of cathodic potential leads to the reduction of species adsorbed on the cathodic surface and causes the formation of the products catalyzing

chemical reaction with participation of citrate as reducing agent. The changes of the catalytic activity of the cathodic surface result in fading of the chemical reactions and reducing the AFE with deposition time. The detailed discussion of this phenomenon is reported elsewhere.<sup>13</sup> Here it is necessary to emphasize the entirely different characters of the deposition time dependences of the FE in the stirred electrolytes containing different concentrations of citric acid and the similarity of these dependencies in the stagnant electrolytes. This similarity suggests that in the stagnant electrolytes with 100 mM and 340 mM citric acid, identical species consisted of a  $\text{Ni}^{2+}$ -citrate complex and  $\text{ReO}_4^-$  are adsorbed on the cathode surface. The closeness of Re-contents (60–65 at.%, cf. Table I) in the deposits produced from the stagnant electrolytes with different concentrations of citric acid confirms this suggestion.

It is known that in the range of pH 4–7 at low concentrations (10 mM and less) of the metal ion and ligand, the dominant form is citrate complex with negative charge of the type  $[\text{NiCit}]^-$ , although the neutral  $[\text{NiHCit}]^0$  complex is also present.<sup>20–23</sup> The formation of  $[\text{NiHCit}]^0$ ,  $[\text{NiCit}]^-$ ,  $[\text{Ni}_2\text{Cit}(\text{H}_{-1}\text{Cit})_3^-]$ , and  $[\text{Ni}_2(\text{H}_{-1}\text{Cit})_2]_4^-$  complexes was shown at high  $\text{Ni}^{2+}$  and citrate concentrations comparable with those used in industrial electrolytes and over a wide range of solution acidity.<sup>23</sup>

We believe that AFE values of 100–125% observed in the deposition for 2–5 s (Fig. 2b) in the stagnant electrolytes are associated with simultaneous reduction of adsorbed  $[\text{NiCit}]^-$ - $\text{ReO}_4^-$  species and with the catalytic effect of their reduction products on the parallel chemical reactions as discussed above.

The species transported to the cathode in the stirred electrolytes form the adsorbed layer with the composition differed from that existed in the stagnant electrolytes. The composition of the adsorbed layer is influenced by the  $\text{Ni}^{2+}$ -complexes presented in the electrolyte and by the relative rates of their and  $\text{ReO}_4^-$  ions transport, and species adsorption on the cathode. In the stirred electrolytes containing 100 mM citric acid, the higher values of AFE (about 220%) are, presumably, associated with the prevailing deposition of Ni from  $[\text{NiCit}]^-$ . This statement is consistent with the formation of Ni-rich alloys at the given  $\text{Ni}(\text{SO}_3\text{NH}_2)_2$  and  $\text{NH}_4\text{ReO}_4$  concentrations (Table I).

The decrease of the efficiency of Ni deposition with the increase of the concentration of citric acid may be explained by the decreased concentration of free  $\text{Ni}^{2+}$  cations in the electrolyte in the presence of high concentration of complexing agent.<sup>12,23,24</sup> At pH5, the formation of  $\text{Ni}^{2+}$  binuclear complexes of the types shown above may contribute to decrease of free  $\text{Ni}^{2+}$  cations.<sup>23</sup>

In the stirred electrolytes containing 340 mM citric acid, the very low FE of the deposition process and 100% Re-content in the deposits can be explained by the difficulty of Ni deposition as a result of the low concentration of free  $\text{Ni}^{2+}$  ions and, probably, by primary  $\text{ReO}_4^-$  transport to the cathode and its adsorption on its surface.

*Effect of stirring on the composition of Re-Ni alloys.*— In the present section of the paper, we consider the effect of the electrolyte stirring on the composition of the Re-Ni alloys produced in relatively long deposition. Under such conditions, the chemical reactions are fading and the system has reached its steady-state condition, characterized by FE and Re-content independent on the deposition time (See Ref. 13 and Fig. 2).

The following results were obtained for electrodeposition from the electrolytes containing 340 mM citric acid for 900 s.

- When electrodeposition was carried out in stirred and stagnant electrolytes containing 94 mM  $\text{Ni}(\text{SO}_3\text{NH}_2)_2$  and 10 mM  $\text{NH}_4\text{ReO}_4$ , the Re-content in the deposits was found to be 78 at.% and 58 at.%, respectively.
- In the stagnant electrolytes containing 17 mM  $\text{Ni}(\text{SO}_3\text{NH}_2)_2$  and 34 mM  $\text{NH}_4\text{ReO}_4$ , about 15 at.% Ni co-deposited. In the deposits produced in the stirred electrolytes containing 17–68 mM  $\text{Ni}(\text{SO}_3\text{NH}_2)_2$  and 34 mM  $\text{NH}_4\text{ReO}_4$ , no Ni was found (i.e. the

**Table I.** The effect of mass transport on the faradaic efficiency and Re-content at different concentrations of citric acid. All electrolytes contained 94 mM Ni(SO<sub>3</sub>NH<sub>2</sub>) and 34 mM NH<sub>4</sub>ReO<sub>4</sub>, pH = 5.

Citric acid content, mM	Dep. time, seconds	Stirred electrolyte		Stagnant electrolyte	
		Re, at%	FE, %	Re, at%	FE, %
100	30	35	98	65	60
100	900	30	95	60	55
340	150	100	5	65	50

deposits contained 100 at.% Re). When the concentration of Ni<sup>2+</sup> was increased to 100 mM, codeposition of 8 at.% Ni was observed.

These data support the results shown in Table I. Thus, mass transport contributes to the increase of Re-content in deposits produced from electrolytes with 340 mM citric acid. This regularity is consistent with the concept discussed in the previous section.

*The effect of mass transport on AFE at low pH.*— The species and their relative concentrations presented in the Ni citrate electrolytes at pH 3 and pH 5 are different. Although at pH 3 H<sub>3</sub>Cit and (H<sub>2</sub>Cit)<sup>-</sup> ions dominate in solutions of citric acid,<sup>20,21,24</sup> the (NiCit)<sup>-</sup>, (NiHCit)<sup>0</sup> complexes and free Ni<sup>2+</sup> ions exist in nickel citrate electrolytes. The (NiCit)<sup>-</sup> complex does not dominate at pH 3 unlike at pH 5 and higher pH values.<sup>21–23</sup> The fraction of the (NiH<sub>2</sub>Cit)<sup>0</sup> species does not exceed 2% of the total stoichiometric concentration of the Ni<sup>2+</sup> ion.<sup>24</sup> In view of the different distribution of species at pH 3 and its possible influence on the deposition process, the study of AFE at pH 3 and its response to the electrolyte stirring is of interest.

The deposition in the stirred electrolytes containing 100 mM citric acid at pH 3 is characterized by low values of the AFE, while the AFE for deposition in stagnant electrolytes is high (Table II). The data in Table II show that, in the stirred electrolytes at pH 3, the AFE does not exceed 25%, while in stagnant electrolytes it can be much higher than 100% and decrease with deposition time.

The decrease of FE with the decreasing pH is not surprising and is observed in deposition of the different Ni alloys (for example, see Refs. 23 and 24). This regularity is easily explained by the enhanced concentration of protons and by the decrease of the concentrations of other electroactive species at the cathode surface. However, no decrease of AFE in stagnant electrolytes at pH 3 was observed. In opposite, the comparison of the values in Table II with the data in Fig. 2b showed that AFE in stagnant electrolytes was higher at pH 3 than at pH 5 (180–110% vs 125–75% for the deposition time 2–10 s).

As discussed above, the AFE observed in stagnant electrolytes can be explained by the formation of a catalytic layer obtained from the [NiHCit]<sup>0</sup>-ReO<sub>4</sub><sup>-</sup> species, after application of current and shift of potential. The lower stability of the [NiHCit]<sup>0</sup> complexes compared to the [NiCit]<sup>-</sup> complexes<sup>24</sup> and parallel deposition of Ni from the [NiHCit]<sup>0</sup> can explain the AFE values exceeding those observed at pH 5 in stagnant electrolytes. In stirred electrolytes, H<sup>+</sup> ions replace the [NiHCit]<sup>0</sup>-ReO<sub>4</sub><sup>-</sup> species on the cathode surface. This situation leads to low FE as was observed in our experiments (Table II).

The results of the electrochemical experiments reported in the present paper are consistent with the assumption of formation of a catalytic layer from species containing Ni-citrate complex with ReO<sub>4</sub><sup>-</sup>

**Table II.** The Effect of mass transport on the Faradic efficiency (%) for electrolytes containing 100 mM citric acid, 94 mM Ni(SO<sub>3</sub>NH<sub>2</sub>) and 34 mM NH<sub>4</sub>ReO<sub>4</sub>, pH = 3.

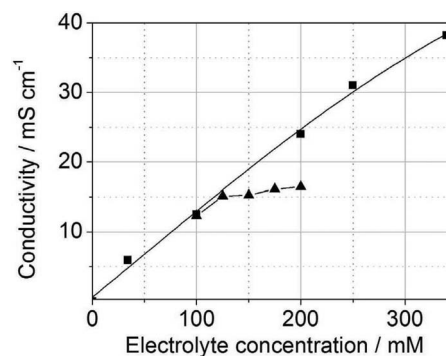
Deposition time, seconds	AFE, %	
	Stirred electrolyte	Stagnant electrolyte
2	8	180
5	21	144
10	23	110

ion. The following sections of the paper are devoted to studying interaction between Ni-citrate complex and perrhenate by conductometry, UV-Vis and Raman spectroscopy.

*Conductometry.*— The results of conductometry of the different electrolytes are shown in Fig. 3 and Table III. It is evident that the specific conductivity  $\sigma$  of the citric acid solutions at pH 5 increased with concentration in the range considered (Fig. 3). As found for many electrolytes, ionic interactions at high ionic concentrations retard the rate of increase of  $\sigma$ , and even produce a decrease of  $\sigma$ . For example, for sodium citrate, a maximal value of  $\sigma = 57.7 \text{ mS cm}^{-1}$  was reached in a 1.099 M solution.<sup>25</sup>

The value of  $\sigma$  of the Ni citrate electrolytes (containing 100 mM citric acid) increased only slightly with increasing Ni sulfamate concentration up to 100 mM. In an electrolyte containing 100 mM citric acid and 100 mM Ni sulfamate it is only  $16 \text{ mS cm}^{-1}$ , while its value for a 200 mM citric acid solution is  $24 \text{ mS cm}^{-1}$ . Increasing the concentration of Ni<sup>2+</sup> to 128 mM increases the value of  $\sigma$  significantly, to  $21 \text{ mS cm}^{-1}$ . This increase is considerably higher than could be expected from the slope of  $\sigma$  dependency on the molar concentration in the range of 0–100 mM Ni sulfamate, and occurs because there are at least 28 mM free Ni<sup>2+</sup> ions in solution. This is consistent with the well-known fact that nickel forms complexes with citrate and, as long as the citrate concentration exceeds that of nickel sulfamate, there are no free Ni<sup>2+</sup> ions in solution. The observed variation of  $\sigma$  is in good agreement with its variation observed in other electrolytes, where complexes are formed.<sup>26,27</sup> It should be noted, however, that the above statement is valid for conditions under which our experiments were conducted and particularly at pH  $\geq 5$  where there are practically no neutral citric acid molecules in solution.

The values of  $\sigma$  for the electrolytes for deposition of Ni and Re-Ni of equal total molar concentrations are reported in Table III. The total concentrations were 228 mM and 468 mM for electrolytes containing 100 mM and 340 mM citric acid, respectively. No noticeable change of  $\sigma$  was observed as a result of the partial replacement of Ni sulfamate for equivalent amount of ammonium perrhenate, both for electrolytes containing 100 mM and 340 mM citric acid. Thus, the results of conductometry did not indicate Ni-citrate complex and perrhenate interaction, while Ni<sup>2+</sup> and citrate interaction was shown.

**Figure 3.** Specific conductivity of electrolytes vs. their molar concentrations. Citric acid solutions (■); electrolytes containing 100 mM citric acid and 0–100 mM Ni(SO<sub>3</sub>NH<sub>2</sub>)<sub>2</sub> (▲). All tests were done at pH = 5.0 ± 0.1.

**Table III. The effect of electrolyte composition on its conductivity.**

Ni <sup>2+</sup> , mM	ReO <sub>4</sub> <sup>-</sup> mM	Citrate, mM	(Ni <sup>2+</sup> + ReO <sub>4</sub> <sup>-</sup> )/ citric acid	Electrolyte concentration (Ni <sup>2+</sup> + ReO <sub>4</sub> <sup>-</sup> + citric acid), mM	Specific conductivity, mS cm <sup>-1</sup>
94	34	340	0.376	468	44
128	—	340	0.376	468	45
94	34	100	1.28	228	22
128	—	100	1.28	228	21

**UV-Vis spectroscopy.**— Figure 4a shows the UV spectra of an electrolyte containing 34 mM ReO<sub>4</sub><sup>-</sup>, 94 mM Ni<sup>2+</sup> and 340 mM citric acid (dashed line), of an electrolyte containing both perrhenate and citric acid (dotted line), and of an electrolyte containing Ni<sup>2+</sup> and citrate (solid line). The spectrum for the electrolyte containing nickel salt and citric acid exhibits three peaks: at 384 and 635 nm in the visible range, and at 233 nm in the UV range. The presence of perrhenate has no effect on the position and height of the peaks in the visible range, which are characteristic of the Ni<sup>2+</sup> complexes in the presence of citrate.<sup>11,12,21</sup> No indication of a ternary Ni<sup>2+</sup>-ReO<sub>4</sub><sup>-</sup>-citrate complex was found. This is consistent with the conclusions of other authors.<sup>11</sup>

The UV spectra of the electrolytes containing perrhenate (with and without nickel) exhibit a single peak at 250 nm. The position and the values of the peaks in the UV range cannot be used for analysis, because of the poor resolution of the spectrometer at high absorbance (higher than about 1.5), which does not allow us to distinguish between the peaks related to different components.

ReO<sub>4</sub><sup>-</sup> absorbs light in the UV range with a maximum at 225 nm.<sup>28</sup> We observed the shoulder near this wavelength for dilute solution containing 0.34 mM ReO<sub>4</sub><sup>-</sup> and 0.34 mM citrate (Fig. 4b). The peak at 205 nm corresponds to absorption by the carboxylate groups of citric acid.<sup>29</sup> The absorbance values observed for the electrolytes for Re and Re-Ni deposition are considerably higher than those suitable for analysis. Unsuccessful attempts to characterize ReO<sub>4</sub><sup>-</sup>-citric acid complexes by UV-Vis absorption spectroscopy were reported before.<sup>11,19</sup>

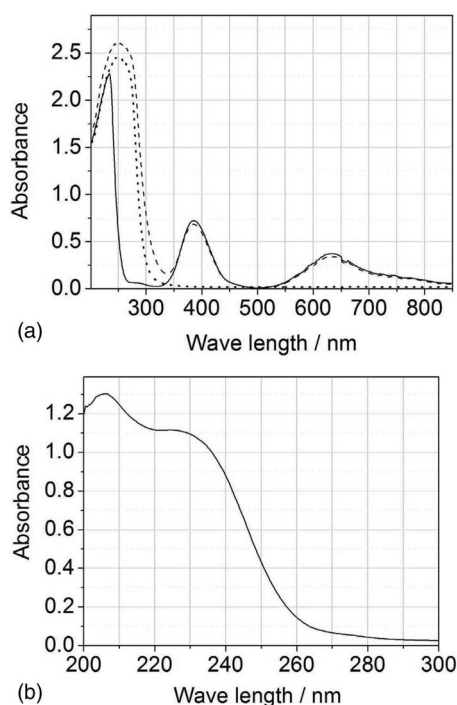


**Figure 4.** UV-Vis spectra of electrolytes. (a) — 340 mM citric acid and 94 mM Ni(SO<sub>3</sub>NH<sub>2</sub>)<sub>2</sub>; - - - 340 mM citric acid, 94 mM Ni(SO<sub>3</sub>NH<sub>2</sub>)<sub>2</sub> and 34 mM NH<sub>4</sub>ReO<sub>4</sub>; ····· 340 mM citric acid and 34 mM NH<sub>4</sub>ReO<sub>4</sub>. (b) 0.34 mM citric acid and 0.34 mM NH<sub>4</sub>ReO<sub>4</sub>.

**Raman spectroscopy.**— Raman spectroscopy was first applied here, to the best of our knowledge, for studying electrolytes for Re-Ni deposition. In order to estimate the effect of simultaneous presence of Ni(SO<sub>3</sub>NH<sub>2</sub>)<sub>2</sub> and NH<sub>4</sub>ReO<sub>4</sub> in citrate electrolyte on the Raman spectrum, we considered the spectra of citrate solution and of citrate electrolytes containing Ni(SO<sub>3</sub>NH<sub>2</sub>)<sub>2</sub> and NH<sub>4</sub>ReO<sub>4</sub> separately.

The addition of NiCl<sub>2</sub> to aqueous sodium citrate solution causes changes in the Raman spectra, which were shown to be the result of Ni<sup>2+</sup>-citrate complex formation.<sup>30</sup> The Raman wavenumbers obtained in the current work for citrate solutions with and without Ni<sup>2+</sup> are rather different from those reported in Ref. 30, as a consequence of the different concentrations, pH and type of Ni salts used in the two cases. However, the effect of Ni<sup>2+</sup> addition is similar to that observed in Ref. 30. Our observations are listed below:

- (i) Appearance of the additional O-C-O deformation bands at 425, 476, 560, 578 and 680 cm<sup>-1</sup> (it is difficult to define their exact position because of their very low intensities and large width).
- (ii) Shift in the O-C-O deformation at 841.5 to 847.5 cm<sup>-1</sup>.
- (iii) Shift of the C-C symmetric stretch at 900 and 950 cm<sup>-1</sup> to 910 and 955 cm<sup>-1</sup>, respectively.

Our results are consistent with those obtained in Ref. 30, showing the formation of [NiCit]<sup>-</sup> complex.

Three fundamentals have been observed for the ReO<sub>4</sub><sup>-</sup> anion in aqueous solutions: at 971, 916 and 332 cm<sup>-1</sup>. They are attributed to symmetric stretching of the Re = O, asymmetric stretching of Re = O, and deformation of O-Re-O, respectively.<sup>31-34</sup> We observed the same bands in the spectra for aqueous solutions of NH<sub>4</sub>ReO<sub>4</sub> at pH 5.

The band near 400 cm<sup>-1</sup> in the spectra of electrolytes containing 340 mM citric acid was transformed to a wide band near 380–410 cm<sup>-1</sup> in the spectra of electrolytes containing 340 mM citric acid and 34 mM NH<sub>4</sub>ReO<sub>4</sub>. The weak peak at 900 cm<sup>-1</sup>, corresponding to C-C stretching, could not be observed, because of superposition of the Re = O asymmetric stretching peak at 922 cm<sup>-1</sup> and formation of a wide band near 912–922 cm<sup>-1</sup>. The O-C-O deformation at 841 cm<sup>-1</sup> and C-C symmetric stretch at 954 cm<sup>-1</sup> of citrate were virtually unaffected by the presence of ReO<sub>4</sub><sup>-</sup>. The shifts of ReO<sub>4</sub><sup>-</sup> vibration bands did not exceed 3 cm<sup>-1</sup>. Based on the results obtained we could not state unambiguously that a complex of ReO<sub>4</sub><sup>-</sup> with citrate is formed.

Upon addition of 94 mM Ni(SO<sub>3</sub>NH<sub>2</sub>)<sub>2</sub> to an electrolyte containing 340 mM citric acid and 34 mM NH<sub>4</sub>ReO<sub>4</sub>, we observed the following features in the spectra, bases on the data in Fig. 5:

- (i) Appearance of weak bands in the range of 422–583 cm<sup>-1</sup>, similar to those observed in the solutions containing 340 mM citric acid and 94 mM Ni(SO<sub>3</sub>NH<sub>2</sub>)<sub>2</sub>. Unfortunately, it is impossible to determine exactly the position of the bands, because of their broadening and low intensity.
- (ii) Shift of the positions of other bands associated with O-C-O and C-C vibrations (at 840 to 847 cm<sup>-1</sup> and at 950 to 954 cm<sup>-1</sup>) to those as in the solutions containing 340 mM citric acid and 94 mM Ni(SO<sub>3</sub>NH<sub>2</sub>)<sub>2</sub>
- (iii) No noticeable differences in the positions of the bands associated with ReO<sub>4</sub><sup>-</sup> vibrations were revealed for the electrolytes containing 340 mM citric acid, 34 mM NH<sub>4</sub>ReO<sub>4</sub> and 94 mM Ni(SO<sub>3</sub>NH<sub>2</sub>)<sub>2</sub>, and for the electrolytes containing 340 mM citric acid, 34 mM NH<sub>4</sub>ReO<sub>4</sub>.

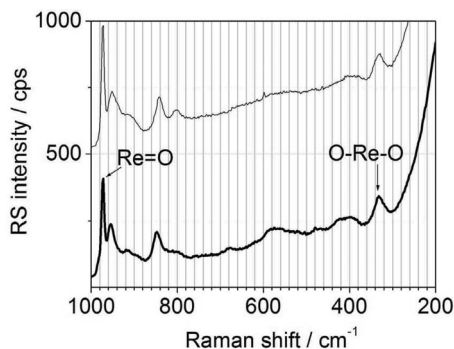


**Figure 5.** The effect of  $\text{Ni}(\text{SO}_3\text{NH}_2)_2$  addition to an electrolyte containing 340 mM citric acid and 34 mM  $\text{NH}_4\text{ReO}_4$  on the Raman spectra. Thin line – no  $\text{Ni}(\text{SO}_3\text{NH}_2)_2$ ; thick line – 94 mM  $\text{Ni}(\text{SO}_3\text{NH}_2)_2$ .

Based on these observations, we can consider the spectra of the electrolytes containing citric acid, perrhenate and  $\text{Ni}^{2+}$  as superposition of the spectra of the electrolytes containing citrate and perrhenate and the electrolytes containing citrate and  $\text{Ni}^{2+}$ . However, the ratio of intensities of the band at  $972\text{ cm}^{-1}$  to that at  $331\text{ cm}^{-1}$  in the spectra of the electrolytes with and without  $\text{Ni}^{2+}$  ions are substantially different, as seen in Fig. 5.

In Fig. 6 we see the effect of  $\text{Ni}^{2+}$  concentration in citrate electrolytes with different concentrations of  $\text{NH}_4\text{ReO}_4$  (17 mM and 34 mM) on the intensity ratio of the bands at  $972\text{ cm}^{-1}$  and  $331\text{ cm}^{-1}$ . As can be seen, the intensity ratio decreased with an increased concentration of  $\text{Ni}(\text{SO}_3\text{NH}_2)_2$ , for both concentrations of  $\text{NH}_4\text{ReO}_4$ .

The increase of the  $\text{ReO}_4^-$  concentration in the electrolytes with constant concentrations of citrate and  $\text{Ni}^{2+}$  resulted in the increase in the ratio of intensities (cf. Fig. 7). Figure 8 illustrates the relationship of the  $\text{Ni}(\text{SO}_3\text{NH}_2)_2/\text{NH}_4\text{ReO}_4$  molar ratio to the intensity ratio of the bands at  $972\text{ cm}^{-1}$  and  $331\text{ cm}^{-1}$ . The intensity ratio decreased with increasing the  $\text{Ni}(\text{SO}_3\text{NH}_2)_2/\text{NH}_4\text{ReO}_4$  ratio, irrespective of the  $\text{Ni}(\text{SO}_3\text{NH}_2)_2$  and  $\text{NH}_4\text{ReO}_4$  concentrations in the different electrolytes.

*Weak ionic interaction.*— The dependency of the ratio of intensities (Figs. 6, 7, 8) attributed to different vibrations in the perrhenate ion indicate the deformation of  $\text{ReO}_4^-$  (and, as a consequence, of  $\text{Ni}^{2+}$ -citrate complex) due to their interactions in the electrolyte. However, the formation of a ternary nickel-citrate-perrhenate complex is not indicated. The formation of complex should be accompanied by the shift and by splitting fundamentals and by appearance of new bands.<sup>32</sup> None of these effects was observed upon addition of Ni salt to the citrate solutions of perrhenate.

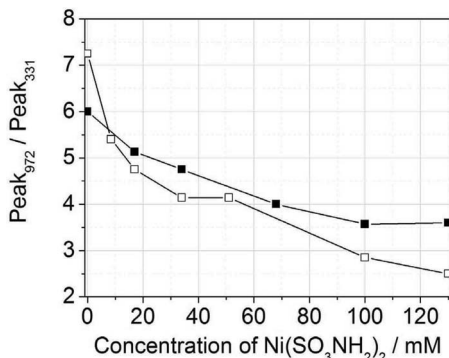


**Figure 6.** The ratio of peak intensities at  $972\text{ cm}^{-1}$  and at  $331\text{ cm}^{-1}$  as a function of  $\text{Ni}(\text{SO}_3\text{NH}_2)_2$  concentration in an electrolyte containing 340 mM citric acid and  $\text{NH}_4\text{ReO}_4$ . 34 mM (■) or 17 mM (□)  $\text{NH}_4\text{ReO}_4$ .

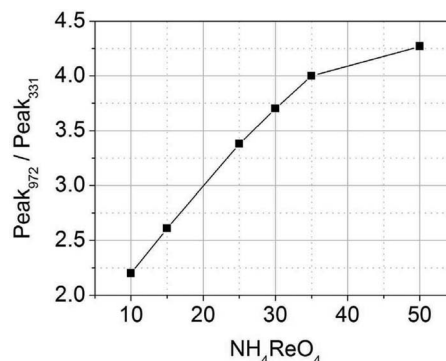


**Figure 7.** The ratio of peak intensities at  $972\text{ cm}^{-1}$  and at  $331\text{ cm}^{-1}$ , as a function of  $\text{NH}_4\text{ReO}_4$  concentration in an electrolyte containing 340 mM citric acid and 94 mM  $\text{Ni}(\text{SO}_3\text{NH}_2)_2$ .

Virtually no significant work has been conducted on formation of complexes of perrhenate in solutions, although weak perrhenate coordination may take place also in aqueous solutions.<sup>32</sup> Recently, it was shown that, in aqueous solutions,  $\text{ReO}_4^-$  behaves as a weak ligand in complex with the uranyl ion ( $\text{UO}_2^{2+}$ ).<sup>35</sup>

The behavior of other oxy-anions, such as  $\text{NO}_3^-$ ,  $\text{ClO}_4^-$  etc. in solutions was studied using Raman spectroscopy, and such phenomena as ion-ion interactions, ion-solvent interaction, formation of ion pairs and outer-sphere complexes could influence the relative intensities of the bands in the Raman spectrum.<sup>36-39</sup> The ratio of Raman intensities is also known to be affected by hydrogen bonding.<sup>40</sup>

Formation of ion pairs of  $\text{ReO}_4^-$  with  $\text{Ni}^{2+}$ -citrate complexes cannot be expected in electrolytes having a molar ratio of citrate/ $\text{Ni}^{2+}$  > 3 at pH 5, as the dominant forms are citrate complex with negative charge  $[\text{NiCit}]^-$  or neutral  $[\text{NiHCit}]^0$  complex.<sup>20-23</sup> In contrast, the formation of ion pairs is possible in solutions without citrate, or with low citrate concentration. As shown by our measurements, addition of  $\text{Ni}(\text{SO}_3\text{NH}_2)_2$  to solutions of perrhenate with 34 mM citrate, or without citrate, did not influence noticeably the ratio of intensities of the peaks at  $972\text{ cm}^{-1}$  and  $331\text{ cm}^{-1}$ . Thus, the interaction responsible for the decrease of this ratio is not associated with ion-pairs formation, and citrate complexes of nickel play an important role in the interactions.

At the present level of our knowledge, it is impossible to determine the nature of this interaction. However, some possibilities could be considered. The relatively large size and low charge density of  $\text{ReO}_4^-$  would make the binding of this ion difficult. The binding of perrhenate could only be achieved by using receptors containing positively charged binding sites. The perrhenate anion can be involved in

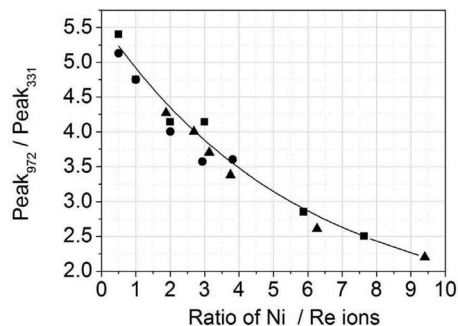


**Figure 8.** The ratio of peak intensities at  $972\text{ cm}^{-1}$  and at  $331\text{ cm}^{-1}$  as a function of the  $\text{Ni}(\text{SO}_3\text{NH}_2)_2/\text{NH}_4\text{ReO}_4$  ratio of molar concentrations in the electrolyte. All electrolytes contained 340 mM citric acid. The  $\text{Ni}(\text{SO}_3\text{NH}_2)_2$  concentration was varied in electrolytes containing 17 mM  $\text{NH}_4\text{ReO}_4$  (■) and 34 mM  $\text{NH}_4\text{ReO}_4$  (●). The  $\text{NH}_4\text{ReO}_4$  concentration was varied in electrolytes containing 94 mM  $\text{Ni}(\text{SO}_3\text{NH}_2)_2$  (▲).

hydrogen bonding with water and such groups as NH- and CH-.<sup>41–44</sup> The increase of the acidity of protons in the receptor contributes to the receptor-perrhenate hydrogen bonding. Besides, binding could arise from pre-organization of the receptor in such a way that it adopts a structure better suited for perrhenate binding.<sup>44</sup> Based on this concept, we could suggest the following way of weak interaction of  $\text{ReO}_4^-$  with  $\text{Ni}^{2+}$ -citrate complex. According to Ref. 30,  $\text{Ni}^{2+}$ -citrate complex includes  $\text{Ni}^{2+}$ , coordinated by 2 ionized carboxylic groups  $\text{COO}^-$  and hydroxyl group of citrate. The combination of  $\text{Ni}^{2+}$  in the complex is expected to increase the acidity of hydrogen in the hydroxyl group and facilitates hydrogen bonding with  $\text{ReO}_4^-$ . This weak interaction changes the coordination of both  $\text{Ni}^{2+}$  and  $\text{ReO}_4^-$  and may be sufficient for the changing the angles between bonds and bond length and strength. These changes are too small to be manifested as a shift in the position of band in UV or Raman spectra or to influence the specific conductivity of the electrolyte, however they may be sufficient for the change in the ability of  $\text{Ni}^{2+}$  and  $\text{Re}^{7+}$  to be reduced.

The new ion coordination on the cathode surface may be more favorable for reduction of both Re and Ni. A similar approach was used for the explanation of the catalytic effect of citric acid on the reduction of  $\text{ReO}_4^-$  on Hg cathode.<sup>19</sup> A weak interaction of  $\text{ReO}_4^-$  with  $\text{Ni}^{2+}$ -citrate complex involves the expansion of the  $\text{Re}^{7+}$  coordination sphere, which could facilitates the reduction of  $\text{ReO}_4^-$ , since the reduced forms of rhenium,  $\text{Re}^{6+}$  or  $\text{Re}^{5+}$  are at least 6-coordinated.<sup>19</sup> The complexes of  $\text{Ni}^{2+}$  can be weakened, when citrate anion forms hydrogen bond with  $\text{ReO}_4^-$  anion.

*Three ways of Re-Ni electrodeposition.*— The deformation of the  $\text{ReO}_4^-$  ion, which is expressed in the changes of the intensity ratio in the Raman spectrum, is a function of the ratio of  $\text{Ni}(\text{SO}_3\text{NH}_2)_2/\text{NH}_4\text{ReO}_4$  (Fig. 8). According to the concept suggested in the previous paragraph, the deformation of ions in their simultaneous presence in the electrolytes facilitates the Re-Ni reduction process and the higher the  $\text{Ni}(\text{SO}_3\text{NH}_2)_2/\text{NH}_4\text{ReO}_4$  ratio, the higher the ionic deformation, and the more intensive is the Re-Ni deposition. This concept could explain the acceleration of Re-Ni deposition when increasing the concentration of  $\text{Ni}(\text{SO}_3\text{NH}_2)_2$  (cf. Fig. 1c). However, it cannot explain the acceleration of Re-Ni deposition when increasing the  $\text{NH}_4\text{ReO}_4$  concentration (cf. Figs. 1a and 1b). According to the data in Figs. 7 and 8, when the  $\text{NH}_4\text{ReO}_4$  concentration increases, the ratio of intensities increases and the ionic deformation has to decrease.

Based on the results obtained here we can suggest the following scenario of induced codeposition of Ni-Re alloys. The electroactive species adsorbed on the cathode include deformed  $\text{ReO}_4^-$  and  $[\text{NiCit}]^-$  ions, with changed coordination of  $\text{Re}^{7+}$  and  $\text{Ni}^{2+}$ . These species present precursor that allow the reduction of  $\text{ReO}_4^-$  and  $[\text{NiCit}]^-$  to proceed simultaneously, enhancing each other. The Re-Ni layer formed in this way seems to catalyze parallel reduction of rhenium from  $\text{ReO}_4^-$ , and reduction of nickel from a  $\text{Ni}^{2+}$ -citrate complex (as well as the chemical reduction reactions with participation of citrate). The acceleration of the Re-Ni deposition process with the increase of  $\text{Ni}(\text{SO}_3\text{NH}_2)_2$  and  $\text{NH}_4\text{ReO}_4$  concentrations (Fig. 1) is associated with the increase of concentrations of the corresponding electroactive ions, which are reduced on the catalytic Re-Ni surface. The level of ionic interaction and deformation on the cathode surface necessary for induced codeposition seems to be significantly lower than that taking place in  $\text{Ni}^{2+}$  concentrations employed in the present work. It is consistent with the fact that even at a ratio of  $\text{Ni}^{2+}/\text{ReO}_4^- = 1/10$ , the catalytic effect of  $\text{Ni}^{2+}$  on the deposition of Re and Re-Ni alloys was observed.<sup>5</sup>

It should be noted that the concept of deposition from three different precursors – Ni-citrate complex,  $\text{ReO}_4^-$  and some species comprising both ions, is consistent with the presence of Re-Ni intermetallic (or alloy) along with pure Re and Ni in the deposits. The detailed discussion of these results obtained by TOF-SIMS method is beyond the scope of the present work and will be presented in a separate publication.

## Conclusions

The regularities of Re-Ni alloy electrodeposition from citrate electrolytes were studied by anodic stripping voltammetry. In order to explain the observed phenomena, the concept of ionic interaction in electrolytes was suggested and verified by conductometry, UV-Visible and Raman spectroscopy.

The increase of the nickel sulfamate and ammonium perrhenate concentrations in the electrolytes was found to intensify the Re-Ni alloy deposition. The composition of the deposit and the time dependency of the anomalous faradaic efficiency (AFE) of the process were found to be strongly influenced by mass transport conditions of the electroactive species and citric acid concentration in the electrolytes.

In stirred electrolytes at pH 5, containing 340 mM citric acid, 94 mM  $\text{Ni}(\text{SO}_3\text{NH}_2)_2$  and 34 mM  $\text{NH}_4\text{ReO}_4$ , a very low FE was observed. The FE increased with deposition time. However, in stirred electrolytes containing 100 mM citric acid, the anomalous FE was found to decrease from about 220% to 95% as the deposition time increased from 2 s to 60 s. The results obtained in stagnant electrolytes with 100 mM citric acid are almost the same as those obtained in the stagnant electrolytes with 340 mM citric acid. The FE decreased from about 125% to 55% when the deposition time increased from 2 s to about 60 s.

High Re-contents (60–65 at.%) were found in the deposits produced in stagnant electrolytes containing both 100 and 340 mM citric acid. Mass transport contributes to the increase of Re-content in the deposits produced in the electrolytes with 340 mM citric acid and contributes to its decrease in the deposits produced in the electrolytes with 100 mM citric acid. The closeness of the FE values and of Re-contents in the deposits produced in the stagnant electrolytes with different concentrations of citric acid implies absorption of some similar species, including a  $\text{Ni}^{2+}$ -citrate complex and  $\text{ReO}_4^-$ , on the cathode surface.

No ternary complexes consisting of  $\text{ReO}_4^-$ ,  $\text{Ni}^{2+}$  and citrate were found in the electrolytes by means of conductometry, UV-Vis and Raman spectroscopy. However, Raman spectroscopy indicated the deformation of perrhenate ions, increasing with increasing the molar ratio of nickel sulfamate and ammonium perrhenate in the electrolytes. This regularity cannot explain the intensification of the deposition process with the increase of  $\text{ReO}_4^-$  concentration in the electrolyte. We conclude that induced co-deposition of rhenium and nickel proceed partially from the precursor adsorbed on the cathode and is partially due to the deformed  $\text{ReO}_4^-$  and  $\text{Ni}^{2+}$ -citrate ions. The deposition from this precursor lead to formation of the layer catalyzing parallel deposition from perrhenate ion and Ni-citrate complex separately.

## Acknowledgments

This research was conducted with financial support from the US Air Force Office of Scientific Research (AFOSR, grant number FA9550–10-1-0520) as well as from the Israel Department of Defense (grant number 4440258441).

## References

1. A. Naor, N. Eliaz, E. Gileadi, and S. R. Taylor, *The AMMTIAC Quarterly*, **5**(1), 11 (2011).
2. L. E. Netherton and M. L. Holt, *J. Electrochem. Soc.*, **98**, 106 (1951).
3. H. Fukushima, T. Akiyama, Y. Toyoshima, and K. Higashi, *J. Met. Finish. Soc. Jpn.* **36**(5), 198 (1985).
4. H. Fukushima, T. Akiyama, Y. Toyoshima, and K. Higashi, *Met. Finish.* **84**(12), 15 (1986).
5. A. Naor, N. Eliaz, and E. Gileadi, *Electrochim. Acta*, **54**, 6028 (2009).
6. A. Naor-Pomeranz, L. Burstein, N. Eliaz, and E. Gileadi, *Electrochem. Solid-State Lett.* **13**(12), D91 (2010).
7. A. Naor, N. Eliaz, and E. Gileadi, *J. Electrochem. Soc.* **157**(7), D422 (2010).
8. A. Naor-Pomeranz, N. Eliaz, and E. Gileadi, *Electrochim. Acta*, **56**(18), 6361 (2011).
9. M. Cohen-Sagiv, N. Eliaz, and E. Gileadi, *Electrochim. Acta*, **88**, 240 (2013).
10. N. Eliaz and E. Gileadi, in *Modern Aspects of Electrochemistry*, Editors, C. G. Vayenas, R. E. White, and M. E. Gamboa-Aldeco, Springer, **42**, 191 (2008).
11. F. Contu and S. R. Taylor, *Electrochim. Acta*, **70**, 34 (2012).
12. M. D. Obradovic, R. M. Stevanovic, and A. R. Despic, *J. Electroanal. Chem.*, **552**, 185 (2003).
13. O. Berkh, N. Eliaz, and E. Gileadi, *J. Electrochem. Soc.*, **161**(5), D219 (2014).

14. P. R. Żabiński, A. Franczak, and R. Kowalik, *ECS Transactions*, **41**(33), 39 (2012).
15. V. A. Makarov, G. M. Florianovich, and Ya. Kolotyrlin, *Fiziko-Khimicheskaya Mekhan. Materialov*, **22**, 3 (1986).
16. S. Swathirajan and Y. M. Mikhail, *J. Electrochem. Soc.*, **136**(8), 2188 (1989).
17. A. Atres and W. Dietzel, *Adv. Eng. Mater.*, **9**, 292 (2007).
18. G. S. Frankel, S. Samaniego, and N. Birbilis, *Corros. Sci.*, **70**, 104 (2013).
19. J. J. Vajo, D. A. Aikens, L. Ashley, D. E. Poeltl, R. A. Bailey, H. M. Clark, and S. C. Bunce, *Inorg. Chem.*, **20**, 3328 (1981).
20. E. Beltowska-Lehman and P. Ozga, *Electrochim. Acta*, **43**(5–6), 617 (1998).
21. O. Yu. Zelenin, *Russian J. Coord. Chem.*, **33**(5), 346 (2007).
22. R.-S. Juang, H.-C. Kao, and F.-Yi Liu, *J. Hazard. Mater. B*, **128**, 53 (2006).
23. D. Golodnitsky, N. V. Gudim, and G. A. Volyanuk, *J. Electrochem. Soc.*, **147**(11), 4156 (2000).
24. O. Younes and E. Gileadi, *J. Electrochem. Soc.*, **149**(2), C100 (2002).
25. H. M. Villullas and E. R. Gonzalez, *J. Phys. Chem. B*, **109**, 9166 (2005).
26. I. P. Makarychev and G. V. Motuzova, *Moscow University Soil Science Bulletin*, **68**(1), 41 (2013).
27. F. Al-Ali, A. Lebugle, I. Rico-Lattes, and G. Etemad-Moghadam, *J. Colloid Interface Sci.*, **289**, 504 (2005).
28. J. W. Atkinson, M.-C. Hong, D. A. House, P. Kyritsis, Y.-J. Li, M. Nasreldin, and A. G. Sykes, *J. Chem. Soc. Dalton Trans.*, **20**, 3317 (1995).
29. M. Donten and J. Osteryoung, *J. Appl. Electrochem.*, **21**, 496 (1991).
30. R. I. Bickley, H. G. M. Edwards, R. Gustar, and S. J. Rose, *J. Molec. Structure*, **246**, 217 (1991).
31. M. A. Vuormant and I. E. Wachs, *J. Phys. Chem.*, **96**, 5008 (1992).
32. M. C. Chkravorti, *Coordin. Chem. Rev.*, **106**, 205 (1990).
33. H. Howard, H. Claassen, and A. J. Zielen, *J. Chem. Physics*, **22**, 707 (1954).
34. L. Wang and W. K. Hall, *J. Catal.*, **82**, 177 (1983).
35. A. Chaumont, O. Klimchuk, C. Gaillard, I. Billard, A. Ouadi, C. Hennig, and G. Wipff, *J. Phys. Chem. B*, **116**, 3205 (2012).
36. Y. A. Makashev and V. E. Mironov, *Russian Chem. Rev.*, **49**(7), 631 (1980).
37. M. Xu, J. P. Larentzos, M. Roshdy, L. J. Criscenti, and H. C. Allen, *Phys. Chem. Chem. Phys.*, **10**, 4793 (2008).
38. R. L. Frost and D. W. James, *J. Chem. Soc. Faraday Trans.*, **78**, 3235 (1982).
39. D. W. James, in *Progress in Inorganic Chemistry*, Editor, S. J. Lippard, John Wiley & Sons, **33**, 353 (1985).
40. A. Nose, M. Myojin, M. Hojo, T. Ueda, and T. Okuda, *J. Bioscience. Bioeng.*, **99**(5), 493 (2005).
41. I. B. Liss and E. O. Schlemper, *Inorg. Chem.*, **14**(12), 3035 (1975).
42. G. Rouschias, *Chem. Rev.*, **74**(5), 531 (1974).
43. U. S. Ray, G. Mostafa, T. H. Lu, and C. Sinha, *Crystal Eng.*, **5**, 95 (2002).
44. E. A. Katayev, G. V. Kolesnikov, and J. L. Sessler, *Chem. Soc. Rev.*, **38**, 1572 (2009).